

THE BUTTERFLY DIAGRAM IN THE 18TH CENTURY

R. Arlt

© Springer

Abstract Digitized images of the drawings by J.C. Staudacher were used to determine sunspot positions for the period of 1749–1796. From the entire set of drawings, 6285 sunspot positions were obtained for a total of 999 days. Various methods have been applied to find the orientation of the solar disk which is not given for the vast majority of the drawings by Staudacher. Heliographic latitudes and longitudes in the Carrington rotation frame were determined. The resulting butterfly diagram shows a highly populated equator during the first two cycles (Cycles 0 and 1 in the usual counting since 1749). An intermediate period is Cycle 2, whereas Cycles 3 and 4 show a typical butterfly shape. A tentative explanation may be the transient dominance of a quadrupolar magnetic field during the first two cycles.

Keywords: Sun: sunspots, Sun: magnetic field

1. Introduction

Sunspots typically appear at latitudes between 10° and 40° heliographic latitude. At the beginning of the solar cycle, latitudes tend to be relatively high, while the appearance locations of sunspots shift to low latitudes as the cycle goes on. A plot of the spot appearance latitudes versus time leads to the butterfly diagram (Maunder, 1904). The diagram is typically plotted starting in 1874 with the Greenwich drawings of the solar disk. The shape of the appearance latitude as a function of time has not significantly changed since. Regular updates of the butterfly diagram are provided by Hathaway in publications and in the Internet (see e.g. Hathaway *et al.*, 2003).

It is desirable to extend the butterfly diagram into the past. Especially after the Maunder minimum, the butterfly diagram may tell us about the characteristics of the solar dynamo when it was coming back to normal after an activity lull with very few sunspots seen between 1645 and 1715.

There is a considerable set of drawings of the solar disk made by Johann Staudacher from 1749 to 1796. The total set of 848 drawings were digitized and

¹ Astrophysikalisches Institut Potsdam, An der Sternwarte 16, D-14482 Potsdam, Germany email: rarl@aip.de

described by Arlt (2008, hereafter Paper I). The drawings contain information about 1031 days in the above period, with several days combined in one drawing, and notes about days when nothing was seen (the number has slightly increased since Paper I, because of additional notes taken into account). For 999 of them, sunspots were plotted. Note that Wolf (1857) was aware of Staudacher drawings and counted the sunspots for his sunspot number time series which is still used today. But the positions have never been determined since.

In this study, we present sunspot positions for 999 of the drawings by Staudacher and present the first butterfly diagram obtained for the 18th century. Section 2 evaluates the direction of the rotation in the drawings which appeared to have changed during the entire observing period of 47 years. Section 3 deals with the various methods to derive the orientation of the solar equator, and Section 4 describes the actual position measurements once the equator is given. Section 5 shows the results of the coordinate determinations in form of a butterfly diagram and discusses its features and limitations. Finally, Section 6 discusses possible implications for the theory of the solar dynamo.

2. Rotational direction

Even though the rotation is obvious in many sequences of drawings over several days, there is still an ambiguity between a “normal” image and a mirrored, upside-down image. The two cases are geometrically distinct only by the inclination of the solar rotation axis against the ecliptic, which is far less obvious.

While the rotational direction was from right to left – according to a mirrored, upright projection image – in all images until the end of 1760, spots appear to move from left to right starting in 1761. An obvious occasion is already the pair of observations of 1761 Feb 20 and Feb 24. If the images were still projected, north must then be at the lower border. The observation of 1761 May 25 has indeed “Süd” (south) at the upper solar limb.

Did Staudacher stop using the mirrored image of the projection, or did he turn the images by 180° ? The eclipse of 1753 is an upright but mirrored image, just as the sunspot drawings. The eclipse of 1769 is a mirrored image, turned by 180° which is consistent with the upside-down sunspot drawings starting in 1761. The eclipse of 1791 does not show the direction of the motion of the Moon, but the geometry and the indications of south pole and north pole, which are assumed to point to the celestial ones, are very consistent with a mirrored and rotated image, just as it was in 1769.

The assumption of rotated, but still mirrored images is backed up by further annotations with compass directions which are listed in Table 1. These are – together with the lunar motion in solar eclipse drawings – all the indications available, and we assume that all images are mirrored throughout the period of 1749–1796. Before any of the operations described in the following sections, all images were mirrored. The change in orientation may mean that Staudacher used a Keplerian telescope until 1760 and a Gregorian starting in 1761, but this is speculation.

Table 1. Orientation indications given by Staudacher besides solar eclipses.

Date	North	East	South	West
1760 Sep 26	top	right		
1761 May 25			top	
1762 May 04		left	top	
1762 May 05		left	top	
1762 Nov 21	bottom	left		
1762 Nov 23	bottom			right
1770 Jul 10			top-right	
1773 Aug 14	bottom-left	top-left		
1773 Oct 17	bottom-left			
1774 Jun 16	bottom-right	bottom-left		
1774 Jul 10	bottom-left			
1775 Jun 08	bottom-right			
1777 May 31	bottom-right			
1785 Apr 17	bottom-right			

3. Position angles of the disks

There is no single way of fixing the orientation of the drawings. We have to rely on various methods with various uncertainties. An automatic method to obtain the sunspot positions is not applicable. All the sunspot positions have been determined manually with a few IDL routines specially programmed for the Staudacher images, and the knowledge about how sunspot groups typically appear on the sun (today). The various ways of obtaining the solar equator are described in the following subsections. Four IDL programmes were written for the methods in Sections 3.1, 3.2, 3.4, and 3.5.

3.1. Rotation fitting

The method which is very frequently used in this study is the rotational fitting of observations which are a few days apart. If these show at least two common sunspot groups, the two disks can be turned against each other, in order to achieve a pattern motion consistent with the solar rotation. The more sunspot groups are common to the drawings of both days, the more reliable is the fit.

Due to the possible drawing errors by Staudacher, a fully automatic fit has not been applied. Given two images with not more than about 6 days time difference, one associates spots on one image with spots on the other. The optimum position angles for both drawings is determined numerically from these spot pairs. If more than one pair is available, there is, in general, a unique best fit. Figure 1 shows an example of superimposed drawings of two consecutive days. The spots coming from 1767 Sep 03 are dark grey, the spots of 1767 Sep 04 are shown in lighter grey. The second drawing is rotated in order to match the spot motion best.

We denote individual spot positions in the n -th drawing by Staudacher with $L_i^{(n)}(\phi^{(n)})$, $B_i^{(n)}(\phi^{(n)})$ where i runs over the spots drawn for a specific day. These

are functions of the actual position angle $\phi^{(n)}$ chosen for the transformation of pixel coordinates into heliographic coordinates. The longitudes L_i refer to the center-of-disk meridian until we get to the Carrington frame in Subsection 4.2. We use $n = 1$ and $n = 2$ referring to any given pair of drawings in the following. We need to find the optimum position angles $\phi^{(1)}$, $\phi^{(2)}$ for any pair of images chosen.

The optimization requires a solar surface rotation profile, and we base the following procedure on the sidereal rotation frequency

$$\Omega_{\text{sid}}(B) = 14.358 - 2.87(\sin^2 B - \sin^2 15^\circ) \quad (1)$$

in degrees per day, which was derived using sunspot positions, and where B is the heliographic latitude (Balthasar, Vazquez, and Wöhl, 1986). We approximate the synodic rotation frequency by $\Omega_{\text{syn}} = \Omega_{\text{sid}} - 0.9867 - 0.0333 \cos(\lambda_\odot - 283.4)$, where λ_\odot is the solar longitude of the observing time. In the following, the synodic period $P = 360^\circ/\Omega_{\text{syn}}$ is used.

A modified least squares fit delivers the best choice of the two position angles. For any given pair of $\phi^{(1)}$ and $\phi^{(2)}$, the positions $(L_i^{(1)}(\phi^{(1)}), B_i^{(1)}(\phi^{(1)}))$ and $(L_i^{(2)}(\phi^{(2)}), B_i^{(2)}(\phi^{(2)}))$ are computed. In defining a norm for the optimization, the latitude differences were chosen to enter the error sum with a fourth power rather than as squares in order to give higher weight to the latitudinal fit as compared with the longitudinal one. Since the rotation profile – only known precisely from the last ~ 120 yr – may have been slightly different in the past, it is wise to give lower weight to the rotation period. The resulting position angles also looked subjectively better fitted than with equal powers. The square longitude differences are compared with the theoretically expected longitude shift ΔL_{theor} according to (1):

$$\Delta L_{\text{theor}} = \frac{2 \cdot 360^\circ \Delta t}{P(B_i^{(1)}) + P(B_i^{(2)})}, \quad (2)$$

where Δt is the time difference between the two observations. The equation shows that the average rotation period according to the two different latitude representations is used. The function which is actually minimized is thus

$$f(\phi_1, \phi_2) = \sum_i \left(B_i^{(1)} - B_i^{(2)} \right)^4 + \cos^2 B_{\text{avg}} \left(L_i^{(1)} - L_i^{(2)} - \Delta L_{\text{theor}} \right)^2, \quad (3)$$

All these coordinates B , L , and L_{theor} depend on the position angles $\phi^{(1)}$ and $\phi^{(2)}$ which are varied in order to find the best fit. Since for arbitrary position angles, the corresponding latitudes of the same spot in the two different drawings are not the same, we use B_{avg} as the average of these two “representations”.

3.2. Rotation matching

There are quite a few occasions when there is at least a pair of dates for which a single spot is drawn. If these are directly stacked with transparency, one may

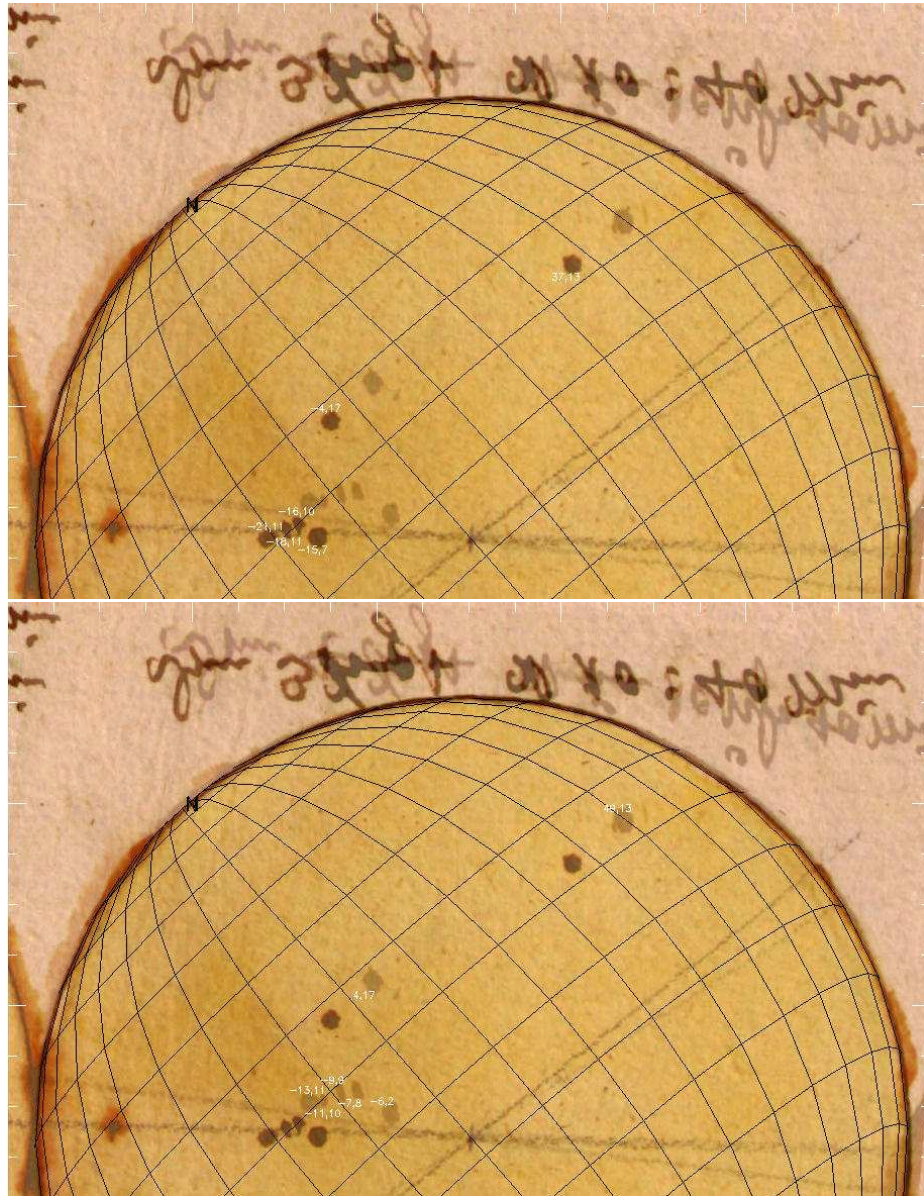


Figure 1. Rotation matching example of the two superimposed drawings of 1767 Sep 3 (dark spots in top panel) and 4 (grey spots in bottom panel). The images are rotated against each other, and scaled to have the same size. Note that all images were mirrored since they are the result of the projected Sun.

have the impression that the equator is indicated by their connection line. But again, the position angles of the two drawings may differ (and they do severely). The rotation matching applied here is a special case of a rotation fit and delivers from zero to two exact solutions for the position angles.

Let us consider the position angle $\phi^{(1)}$ of the first drawing. At a given $\phi^{(1)}$ there are generally two position angles $\phi^{(2)}$ of the second drawing for which the spot falls onto the same latitude as in the first drawing. The azimuthal difference between the longitude $L^{(1)}$ in the first drawing and the longitude $L^{(2)}$ in the second drawing plus the time difference between the two observations gives us a measure for the corresponding rotation period.

The $\phi^{(2)}$ for which the “rotation period” is closest to the expected rotation period according to Balthasar, Vazquez, and Wöhl (1986) is selected and delivers $P_{\text{match}}(\phi^{(1)})$. The other match is discarded. This search of $\phi^{(2)}$ for a given $\phi^{(1)}$ is repeated for all possible $\phi^{(1)} = 0$ to 2π . The “rotation periods” obtained are compared with the true rotation period (assuming it has not changed significantly since the 18th century). A function $P_{\text{match}}(\phi^{(1)}) - P(B)$ is obtained, where B is again the heliographic latitude (note that B in both drawings are equal now). This can have a single minimum where there is an $P_{\text{match}}(\phi^{(1)})$ getting close to P , or it can have two exact solutions where the period difference vanishes. If two solutions matching the rotation period of the corresponding latitude exactly are found, the one for which sunspot latitudes fall below 50° was chosen. This also includes additional spots in the drawings which have no counterpart in the other image. This makes the final result a bit less objective, but the increase in the number of available observations was considered more important.

3.3. Direction lines

A number of drawings show lines drawn by pencil apart from a horizontal line often appearing to align images in rows in the book. There is a total of 188 days for which such additional lines are drawn; most of them are not annotated. Eight of them have markings referring to the ecliptic, 10 others have compass directions as annotations (plus the first four drawings in Table 1 with compass directions but no lines). These are too few to conclude anything about the value for finding the orientations of the drawings; some of them even contradict the distribution of the spots so drastically, that we assume they are not meaningful for our purposes. The lines might not even be inserted by Staudacher himself actually.

3.4. Alignment by sunspot groups

As long as solar activity is not at minimum, the orientation of sunspot groups often provides a fairly accurate guess of the solar equator, especially if there are two or more groups. The uncertainty essentially comes from the statistics of the tilt angles of groups themselves. Howard (1996) determined the average group tilt against the equator to be about 4° , with the preceding spots being closer to the equator than the following ones. The scatter, however, is about 25° around that value. A single group thus provides limited orientation accuracy, but a second group decreases the uncertainty a lot.

3.5. Orientation by time of day

Finally, the drawings also indicate that Staudacher often placed his drawing paper fairly well aligned with the horizon behind the telescope. Times of day are given for observations starting in 1760. Starting with 1763, the orientations appear to be consistent enough with an angle with the horizon. We start using this indication of the drawing orientation occasionally – if no other way of determining the position angle was available – in 1763 first. There was no common reference time in Europe in the 18th century yet, because of the lack of communication means. People in cities and villages most likely referred to a reference clock which was adjusted according to astronomical events and thus showed something close to local time. We assumed that Staudacher’s clock times are local time for Nuremberg.

Obtaining the drawing orientation from the time of day is the only method where the geographical location of Staudacher matters. We assume a geographical longitude of $\lambda = 11.08^\circ$ W and latitude of $\phi = 49.45^\circ$ N for the spherical transformations. The total position angle of the solar rotation axis against the direction to the zenith is determined from the tilt of the celestial equator against the horizon, the tilt of the ecliptic against the equator, and the tilt of the solar equator against the ecliptic for the given date and time. The orientations of 173 drawings were primarily based on the time of day. For other drawings, if for example the spot distribution was used primarily, the time of day helped as an additional support of other estimates made for the solar equator.

3.6. Additional remarks

The partial solar eclipse of 1769 June 4 was noted as observed on June 3. This seemed to indicate that Staudacher used astronomical dates starting at noon (cf. Paper I). However, the spot motion on consecutive days has nowhere shown a discrepancy with dates starting at midnight. An example is the pair of drawings on 1764 February 16, at 14h, and 1764 February 17, at 10h. While an astronomical day count would imply that these two observations are 1.6 days apart, the spot motion clearly shows that a difference of 0.8 days is much more likely.

In some cases, two position angles were about equally plausible. The sunspot positions of both orientations were kept in the file of positions. The positions are stored in daily blocks separated by blank lines. The results of two position angles are identified by two blocks with the same date (plus verbal remarks). Because of the limited accuracy of the drawings, we are seeking statistical results rather than results on individual spots. When these data are used, one should make sure a considerable set of positions is involved.

4. Sunspot positions

4.1. Heliographic latitudes

Once the orientation of the solar equator is defined, an “observed” heliographic coordinate system is established over the drawing. The following operations have

all been worked out with IDL’s map routines which are part of any recent IDL installation. Note that the drawings are not necessarily precisely circular. Most of the distortions led to elliptical drawings with a longer vertical axis and a shorter horizontal one. The ellipticity is taken into account by measuring both the horizontal and the vertical extent of the circle drawn directly on the screen. Since IDL allows for non-circular spherical grids, the setup of the surface map was straight-forward.

Setting up the coordinate system requires the determination of the tilt of the sun against the observer. Because of the small inclination of the sun’s equator of 7.25° , we can use an approximation for the annual variation of the tilt and apply

$$B_0 = 7.25^\circ \cos(\lambda_\odot + 15^\circ) \quad (4)$$

to obtain the latitude of the center of the solar disk, there λ_\odot is the solar longitude for eq. J2000.0. The error compared with the much more complex IAU2000 rotation model (Seidelmann *et al.*, 2002) is 0.35° at maximum. The error in heliographic longitude is one order of magnitude smaller. The heliographic positions (L_{obs}, B) were then measured on the screen with the pixel accuracy of the digitized images which is between 0.16° and 0.26° in the center of the solar disk depending on the size of the photographic reproductions. Note that the longitude L_{obs} still refers to the central meridian at the time of the observation; the conversion into the Carrington frame is described in the following Subsection.

A subjective quality tag q is assigned to each day, essentially evaluating the quality of fixing the equator. The ranking uses $q = 1$ for very good, $q = 2$ for mediocre quality, and $q = 3$ for unreliable positions. A rotational fitting typically delivers $q = 1$; in a number of cases, the fit was not fully convincing and received $q = 2$. Orientations obtained from group alignments typically have $q = 3$, if several groups were available or the distribution in general supports a particular orientation, the quality was set to $q = 2$. We have to keep in mind though that these position angles are based on the knowledge of spot distribution and roughly horizontal alignment of bipolar groups as they are observed *today*. These characteristics may have been different at Staudacher’s time. The position angles solely taken from the time of day received $q = 3$.

4.2. Heliographic longitudes

The longitudes of all the positions measured refer to the meridian going through the center of the solar disk. The positions need to be converted into the Carrington rotation frame in order to obtain longitudes comparable to modern positional information. We need to compute the heliographic longitude of the center of the solar disk for any given time in 1749–1796. The method described by Meeus (1985) is applied and was implemented in the IDL routines of the Applied Physics Laboratory at Johns Hopkins University (`sun.pro` as of 1991 Jul 24). The algorithm shows slight deviations from the IAU2000 rotation model (Seidelmann *et al.*, 2002) of up to 0.33° when going back to 1749. This is the model used by the HORIZONS ephemerides system at JPL with which we compare here. The

deviation is entirely linear, and we apply a correction

$$L_{0,\text{JPL}} = L_{0,\text{JHU}} + 0.00111(2008 - Y) + 0.041 \quad (5)$$

to the IDL routine, where $L_{0,\text{JPL}}$ and $L_{0,\text{JHU}}$ are the sub-observer heliographic longitudes of JPL and JHU respectively, and Y is the year AD. The heliographic longitude L in the Carrington rotation frame is now simply $L = (L_{\text{obs}} + L_{0,\text{JPL}}) \bmod 360^\circ$. For the observations without any note about the time of day (mostly before mid-1761), local noon was assumed, corresponding to 11h16m UT.

5. The butterfly diagram

The distribution of 6285 sunspot positions versus time and latitude is shown in Figure 2. The duration of spots is set artificially to 50 days in order to increase the visibility of the data without altering the results. Since in this first analysis, only the spot positions were measured and not the individual spot sizes, the latitudinal half-width of the spots is also artificial and was set to $\Delta B = 2^\circ$. The i -th spot at latitude B_i is distributed in latitude b by a simple quadratic function

$$d_i(t, b) = 1 - \left(\frac{b - B_i}{\Delta B} \right)^2, \quad (6)$$

where d_i is a density function of time and latitude; it is set to zero outside $B_i \pm \Delta B$. The spots in Figure 2 thus have a total width of 4° . All these spot densities are added for a single distribution $d(t, b) = \sum_i d_i(t, b)$.

The top panel shows the distribution of all positions measured, i.e. with a quality tag of $q \leq 3$. The middle panel shows only positions with $q \leq 2$ while the lower panel shows $q = 1$ spots exclusively. The times marked with ‘‘Solar activity minima’’ are the times of lowest activity according to the sunspot area measurements presented in Paper I. The minimum times resulting from the Wolf number series may be somewhat different.

The striking feature of Figure 2 is the deviation of the spot distribution from the butterfly shape during the period of 1749–1766. These are Cycles 0 and 1 in the cycle counting based on the Wolf numbers. The solar equator is much more populated by sunspots than we know it today. Also the migration toward lower latitudes is less obvious, especially for Cycle 1 which is well covered by observations. The following Cycle 2 also shows a populated equator but the butterfly shape appears to be already in transition to the typical distribution which is then exhibited by Cycles 3 and 4.

The findings are apparently not altered when selecting only the more reliable positions shown in the middle and lower panel of Figure 2.

6. Discussion

Positional measurements of sunspots observed by Johann Staudacher in the period of 1749–1796 are presented. The data provide us with a butterfly diagram

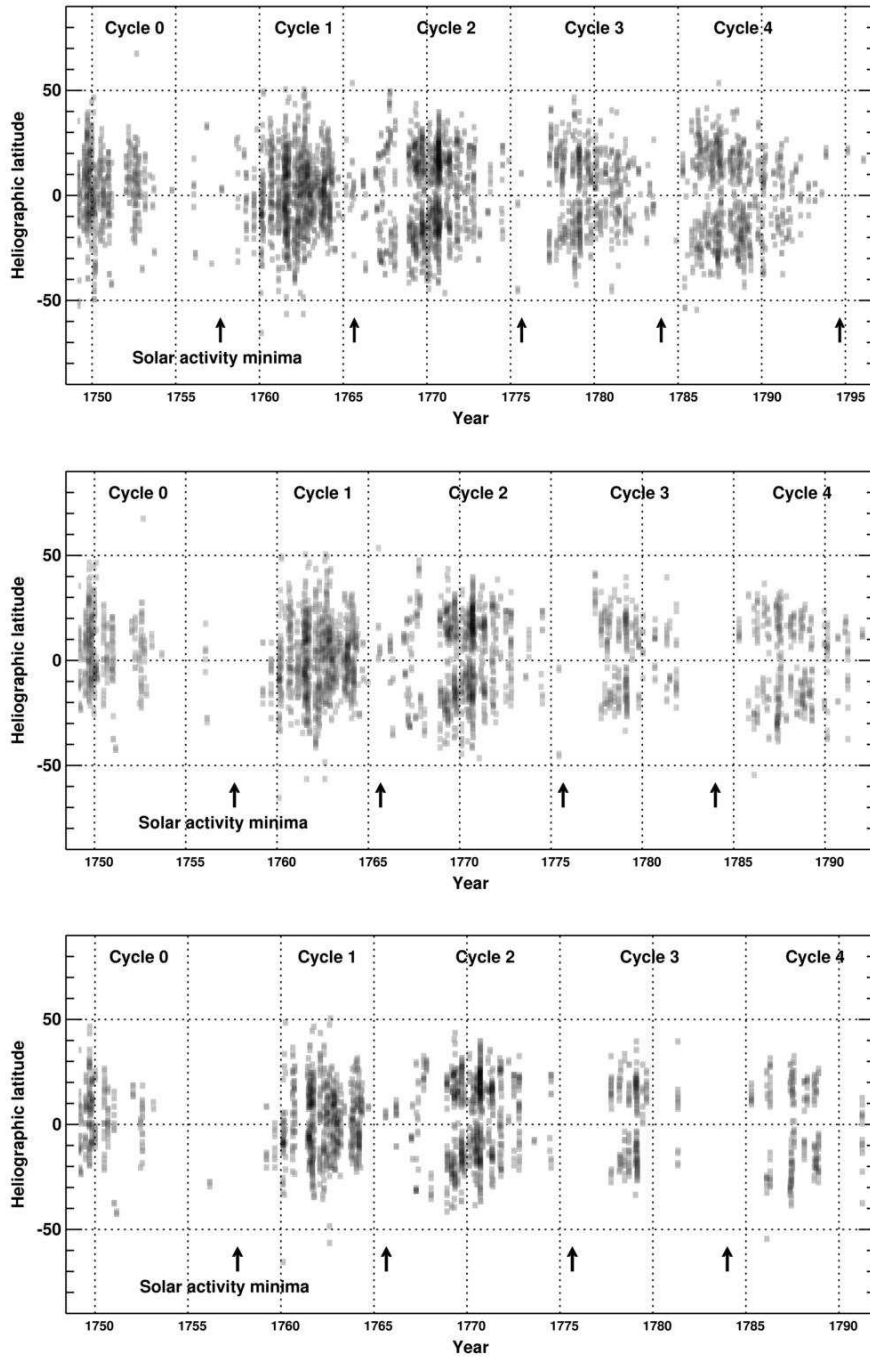


Figure 2. Butterfly diagram as derived from the drawings by Staudacher in 1749–1796. The solar minima were taken from the sunspot area time series of Paper I. The top panels shows all spot positions, the middle panel only spots with medium and high accuracy, the lower panel only high accuracy.

of almost five solar cycles covered. The distribution shows a surprising behaviour. The first two cycles (Cycle 0 and 1) exhibit a different behaviour than the one we know from the “modern” butterfly diagram as recorded since 1874. The highly populated equator indicates the presence of a dynamo mode which is symmetric with respect to the equator. We do not have the magnetic polarities though. Nevertheless, a polarity change across such a populated equator seems very unlikely.

An interesting option is a differential rotation different from today. The assumptions made for the rotational fits and matches will then be less suitable. It is unlikely that the differential rotation changed dramatically during the 18th century, but it will be an interesting topic for future research to actually derive the rotation profile from the spot drawings.

The results presented here may also be affected by a gradual change of observing skills and knowledge of Staudacher. The precise reproductions of the solar eclipses – with the first one drawn in 1753 – indicate, however, that Staudacher projected the image directly on the paper he used for drawing. Such direct copies are likely to be fairly accurate at different stages of knowledge and experience. While there is certainly some development of skill in detecting small sunspots, the positional accuracy should remain fairly constant.

The sunspot cycle has not always shown sunspots as frequent as during the last 250 years. Strongly reduced activity was observed in the Maunder minimum period from about 1645 to 1715. The very few spots were then mostly present on the southern hemisphere (Ribes and Nesme-Ribes, 1993), apart from very few exceptions, until 1711. The cycle near the end of the Maunder minimum starting in about 1713 shows both hemispheres being populated again, with a considerable number of spots below 10° heliographic latitude. Two activity cycles are missing before the results presented here take over. It was recently suggested that the north-south asymmetry may also be relevant for the prolonged Cycle 4 (Zolotova and Ponyavin, 2007).

A number of dynamo models show the appearance of grand minima as a result of nonlinear effects between the magnetic fields and the differential rotation (Tobias, 1997; Küker, Arlt, and Rüdiger, 1999; Bushby, 2006). Recent mean-field models with a meridional circulation controlling the solar cycle have been successful in constructing solar-like activity cycles (Dikpati and Charbonneau, 1999). The butterfly diagram is thought to be a direct consequence of the equator-ward flow at the bottom of the solar convection zone in these models. An interesting fact is the close excitation limits of the dipolar and quadrupolar dynamo modes in these flux-dominated mean-field dynamos (Dikpati and Gilman, 2001). A transient dominance of the quadrupolar (symmetric with respect to the equator) mode can either be explained by the chaotic nature of a deterministic system (Weiss and Tobias, 2001) or by stochastic variations in the turbulence characteristics (Brandenburg and Spiegel, 2008). Such variations have led to distortions of the butterfly diagram very similar to the ones observed by Staudacher in the 18th century. The observations utilized here support the idea that the solar dynamo is modulated by nonlinear interactions between the dipolar mode – dominant at the present time – and a mode of quadrupolar symmetry.

Since the inspection and analysis requires a lot of man power, we have derived here only the positions of the individual spots, but have no information on the sizes of individual spots. There is very likely information still hidden in the individual areas, but we have to postpone these measuring efforts to a future project. The sunspot positions of 1749–1796 are available on request from the author.

Acknowledgements The author is grateful to Jan Meyer for the photographic reproductions of the drawings and to Regina von Berlepsch for the support in the library of the Astrophysikalisches Institut Potsdam. The work also benefited from the support by ISSI, Switzerland, where the utilization of the drawings was discussed in an International Team.

References

- Arlt, R.: 2008, Digitization of Sunspot Drawings by Staudacher in 1749–1796. *Solar Phys.* **247**, 399–410 (Paper I).
- Balthasar, H., Vazquez, M., Wöhl, H.: 1986, Differential rotation of sunspot groups in the period from 1874 through 1976 and changes of the rotation velocity within the solar cycle. *Astron. Astrophys.* **155**, 87–98.
- Brandenburg, A., Spiegel, E.: 2008, Modeling a Maunder minimum. *Astron. Nachr.* **329**, 351–357.
- Bushby, P.J.: 2006, Zonal flows and grand minima in a solar dynamo model. *Mon. Not. Roy. Astron. Soc.* **371**, 772–780.
- Dikpati, M., Charbonneau, P.: 1999, A Babcock-Leighton Flux Transport Dynamo with Solar-like Differential Rotation. *Astrophys. J.* **518**, 508–520.
- Dikpati, M., Gilman, P.A.: 2001, Flux-Transport Dynamos with α -Effect from Global Instability of Tachocline Differential Rotation: A Solution for Magnetic Parity Selection in the Sun. *Astrophys. J.* **559**, 428–442.
- Hathaway, D.H., Nandy, D., Wilson, R.M., Reichmann, E.J.: 2003, Evidence That a Deep Meridional Flow Sets the Sunspot Cycle Period. *Astrophys. J.* **589**, 665–670.
- Howard, R.F.: 1996, Axial Tilt Angles of Active Regions. *Solar Phys.* **169**, 293–301.
- Küker, M., Arlt, R., Rüdiger, G.: 1999, The Maunder minimum as due to magnetic Λ -quenching. *Astron. Astrophys.* **343**, 977–982.
- Maunder, E.W.: 1904, Note on the distribution of sun-spots in heliographic latitude, 1874–1902. *Mon. Not. Roy. Astron. Soc.* **64**, 747–761.
- Meeus, J.: 1985, *Astronomical formulae for calculators*. Willmann-Bell, Richmond, VA, 3rd ed.
- Ribes, J.C., Nesme-Ribes, E.: 1993, The solar sunspot cycle in the Maunder minimum AD1645 to AD1715. *Astron. Astrophys.* **276**, 549–563.
- Seidelmann, P.K., Abalakin, V.K., Bursa, M., et al.: 2002, Report of the IAU/IAG Working Group on Cartographic Coordinates and Rotational Elements of the Planets and Satellites: 2000. *Cel. Mech. Dyn. Astron.* **82**, 83–111.
- Tobias, S.M.: 1997, The solar cycle: parity interactions and amplitude modulation. *Astron. Astrophys.* **322**, 1007–1017.
- Weiss, N.O., Tobias, S.M.: 2000, Physical Causes of Solar Activity. *Space Sci. Rev.* **94**, 99–112.
- Wolf, R.: 1857, Mittheilungen über die Sonnenflecken. *Vierteljahresschrift d. Naturforsch. Gesellsch. in Zürich* **2**, 272–299.
- Zolotova, N. V., Ponyavin, D. I.: 2007, Was the unusual solar cycle at the end of the XVIII century a result of phase asynchronization? *Astron. Astrophys.* **470**, L17–L20.